Progress In Electromagnetics Research C, Vol. 88, 207–218, 2018

Sodium Salt of Polyethylene-Co-Methacrylic Acid Ionomer/Polyaniline Binary Blends for EMI Shielding Applications

Kingsley K. Ajekwene[1, 2, *], Jelmy E. Johny[1], and Thomas Kurian[1]

Abstract—Improvement of properties of polymeric materials through blending is a way to obtain products with highly adapted performance for specific applications. The present work reports the design and preparation of binary blend films of poly(ethylene-co-methacrylic acid) neutralized using sodium salt (EMAANa) and nano polyaniline doped with hydrochloric acid (nano PANI-HCl) or toluene sulfonic acid (nano PANI-TSA) with the aim of achieving improved thermal stability, DC conductivity and electromagnetic interference (EMI) shielding effectiveness (SE) of EMAANa. The binary blends were prepared by solution blending using a solvent mixture of toluene/1-butanol (90 : 10) at 65°C. The hybrid materials were characterized and evaluated by FTIR, UV-Vis spectroscopy, XRD spectroscopy and thermogravimetric analysis (TGA). The electrical conductivity of the PANI and PANI/EMAANa blends was measured by four-probe method. The EMI shielding effectiveness was studied using a waveguide coupled to an Agilent Synthesized Sweeper 8375A and a Hewlett-Packard spectrum analyzer 7000 in the X band frequency range (8–12 GHz). FTIR indicates a π-π and hydrogen bonding interaction between PANI and EMAANa, enabling the PANI to be adsorbed in the ionomer. The TGA of the blends show similar weight loss pattern with nano PANI-TSA/EMAANa exhibiting slightly lower weight loss below the decomposition temperature. The TGA results show that thermal stability of the blends is better compared to pure EMAANa. The results of measurements of electrical conductivity and EMI SE demonstrates that PANI was successfully blended into the EMAANa substrate.

1. INTRODUCTION

Ionomers are polymers containing hydrophobic backbone chains and a small amount of ionic salt groups attached on either the backbones, side chains or on the backbone terminals thereby making it possess polar groups which make it hydrophilic as well. These polar salt groups form ionic aggregations such as mulitplets and clusters making the nonpolar chains to group together and the polar ionic groups to attract and cling to each other [1]. This allows thermoplastic ionomers to act in a way similar to that of crosslinked polymers or thermoplastic elastomers [2, 3]. The ionic attractions strongly affect the polymer properties dramatically; increasing the mechanical properties such as modulus, tensile strength, impact resistance and particularly stiffness [1]. Based on these properties, ionomers are commonly used in commercial and industrial fields including diffusion and electrodialysis, electrolysis, solid polymer electrolyte for batteries, potentiometric sensors, membranes for water treatment, solution recycling and filtering, proton exchange membranes for fuel cells, packaging, coatings, optics, medical and biological fields as sensors, membranes, dental restorative materials, etc. [4]. However, the hydrophilicity due to the introduction of low levels of salt groups (Na^+, K^+, Mg^{2+}, Zn^{2+}, Cu^{2+}, Mn^{2+} and Co^{2+}) makes ionomers loose enormous strength, stiffness and conductivity which is dependent on humidity making ionomers unsuitable for electrical conduction at temperatures below 0°C and above 100°C.

Received 30 September 2018, Accepted 21 November 2018, Scheduled 30 November 2018

* Corresponding author: Kingsley Kema Ajekwene (kemaking@gmail.com).

[1] Department of Polymer Science and Rubber Technology, Cochin University of Technology, Kochi-682022, Kerala State, India.

[2] Department of Polymer and Textile Technology, Yaba College of Technology, P.M.B. 2011, Yaba, Lagos, Nigeria.

Mechanical and electrical properties of polymers are significantly influenced by the presence of fillers such as polyaniline (PANI). By mixing thermoplastics with the electroconducting PANI, besides an increase of electroconductivity, an increase of modulus and tensile strength is expected, accompanied by a decrease of deformability which may result in lower elongation at break and diminished toughness of the material [5].

Polyaniline (PANI) is an electroconductive polymer that has extensive hi-tech uses. Its usage in EMI shielding materials, rechargeable batteries, microelectronics, electrochromic displays, photovoltaic devices, corrosion protection of metals, light-emitting devices, biocompatible materials, catalysts, electrodes, chemical and biological sensors, antistatic coatings, etc. which are primarily due to their light weight, versatility, tunable electrical properties, low cost, environmental stability, redox reversibility and tremendous corrosion resistance, etc., has been amply documented by numerous researchers [6–17]. The intrinsic conductivity of polyaniline makes it a viable material in the field of EMI shielding over wide frequency range of 100 MHz to 20 GHz. In addition, polyaniline exhibits notable EMI shielding through absorption to provide shielding against probable internal EMI which differs from the reflection by metal based shielding mechanism; which makes it fascinating for military applications [14]. However, the insolubility of the doped form, poor mechanical and thermal properties and low processability of PANI have hindered its industrial applications. To overcome these problems, PANI-thermoplastics composite blends are prepared through direct polymerization within a matrix polymer, melt processing and dry mixing such as extrusion, injection or compression moulding and solution processing methods such as casting or spraying by using a suitable solvent and mixing the dispersion with a solution of a matrix polymer [18–23]. This could extend their usefulness and applications in electromagnetic shielding, antistatic charge dissipation, printed circuit boards for electronics applications and corrosion protection of metals such as iron, etc. [24].

In this paper, we report the preparation, characterization and studies on thermal behaviour, DC conductivity and EMI shielding effectiveness of the blends of sodium salt of poly(ethylene-co-methacrylic acid) (EMAANa) and doped nano PANI. Nano polyaniline doped with hydrochloric acid (nano PANI-HCl) or toluene sulfonic acid (nano PANI-TSA) prepared by chemical oxidative polymerization of aniline was blended with the ionomer through a novel solution blending method to obtain a blend with good conductivity and film forming strength. We have adopted solution blending method because it has the advantage of rapid mixing of the system without large energy consumption, the potential to avoid unfavourable chemical reactions, can easily be used for preparation of polymer blends on a laboratory scale and low cost compared to capital intensive mixing method or complex setups for insitu polymerization methods.

2. MATERIALS AND METHODS

2.1. Materials

Ionomers: The ionomer used in this study was supplied by Mitsubishi Plastics, Inc., Japan. [Sodium salt of poly(ethylene-co-methacrylic acid) (HIMILAN 1702 EMAANa) with melt flow index (190°C/2.16 kg) of 16 g/10 min.].

Chemicals and solvents: Ammonium persulphate (APS), toluene sulfonic acid monohydrate (TSA) and aniline obtained from Sigma Aldrich Chemical Company were of very high purity (99.9%). Hydrochloric acid (HCl) 98% and acetone were obtained from Spectrochem Pvt. Ltd, Mumbai, India. The aniline was distilled before use. All other materials were used without any pre-processing.

2.2. Methods

2.2.1. Synthesis of Polyaniline (PANI)

Nano polyaniline was prepared by chemical oxidative polymerization of 200 µl aniline using 0.66 g of ammonium per sulfate dissolved in 1.8 ml water as initiator in the presence of 40 mL aqueous solution of 1 M HCl at room temperature for 12 hrs. The polymer formed was washed with distilled water, dilute HCl solution and finally with acetone in order to remove excess HCl, oxidant, aniline and oligomers and until the filtrate becomes colourless. The green coloured precipitate was then dried in vacuum

oven at 50°C for 24 hours. The dried mass was ground to fine powder using mortar and pestle. The prepared polyaniline is designated as nano PANI-HCl. In order to determine the influence of the novel formulation on the dimensions of the synthesized nano PANI-HCl, polyaniline was also prepared in bulk dimension by polymerizing 20 ml aniline using 66 g of ammonium per sulfate dissolved in 180 ml water as initiator in the presence of 400 ml aqueous solution of 1 M HCl with stirring at room temperature for 12 hrs and designated as bulk PANI-HCl. To confirm the dimensions, the morphologies of both the nano and bulk PANI-HCl were analyzed using SEM.

The same reaction of nano PANI-HCl was repeated with 1 M TSA as dopant keeping all other reactants the same and designated as nano PANI-TSA.

2.2.2. Preparation of Polyaniline-Ionomer Binary Blends

The ionomer (EMAANa) was dissolved in a mixture of 90 : 10-toluene/1-butanol solvents at 65°C. Varying weights (0.1 g, 0.3 g, 0.5 g, 0.7 g, 1.0 g, 1.2 g, 1.5 g and 2.0 g) of the as prepared nano PANI (either nano PANI-HCl or nano PANI-TSA) were mixed thoroughly with ionomer solution to obtain polyaniline-EMAANa binary blends.

A constant weight (1.0 g) each of the EMAANa was used in all the composite blends. The solution of nano PANI/ EMAANa blends were allowed to evaporate to a solid film in a petri dish and dried in vacuum oven at 50°C for 24 hours.

2.3. Characterization and Instrumental Analysis

The morphology and microstructure of the samples was examined by JEOL Model JSM-6390LV SEM and JEOL/JEM 2100 TEM. The Fourier transform infrared (FTIR) spectra of samples were recorded using a Thermo Nicolet Avatar 370 FTIR spectrometer. The compositional state of the samples was determined using X-Ray Powder Diffractometry (XRD-Bruker AXS D8). The optical absorption by the sample in the UV and visible region was measured with Varian Cary 5000 UV-Visible spectrophotometer in the spectral range 225–1000 nm. Thermo gravimetric analysis (TGA) was performed on a Perkin Elmer STA 6000 thermogravimetric analyzer to determine decomposition, transition temperatures and thermal stabilities of the samples. The electrical properties of the PANI samples were measured by four probe technique (D.C conductivity) using sensitive digital electrometer type Keithley Agilent 616. EMI shielding measurements was performed using a wave-guide coupled to an Agilent Synthesized Sweeper 8375A and a Hewlett-Packard spectrum analyzer 7000 in the X band frequency range (8–12 GHz).

3. RESULTS AND DISCUSSIONS

3.1. Scanning Electron Microscopy (SEM)

Figures 1(a), 1(b) and 1(c) show the SEM micrographs of bulk PANI-HCl, nano PANI-HCl and nano PANI-TSA respectively. All the micrographs reveal the irregular granular morphology of the synthesized polyaniline. Bulk PANI-HCl has a porous structure with particle size of 217 nm. The micrographs of nano PANI-HCl and nano PANI-TSA reveal that the synthesized polyaniline comes under nanodimension with an average particle size of 85 nm and 77 nm, respectively.

3.2. Transmission Electron Microscopy (TEM)

The transmission electron micrograph (TEM) images of nano PANI-HCl and nano PANI-TSA are shown in Figures 2(a) and 2(b), respectively. The TEM images clearly show a fibrous like morphology with a diameter of 2 nm in the form of hollow nanorods. The formation of these polyaniline nanorods/nano fibers occurring interfacially at the junction of the organic and aqueous phase during the polymerization process is due to the controlled and limited availability of the aniline monomer. The limited amounts of aniline monomer molecules in the organic phase interacts with the oxidizing agent that is present in the aqueous phase.

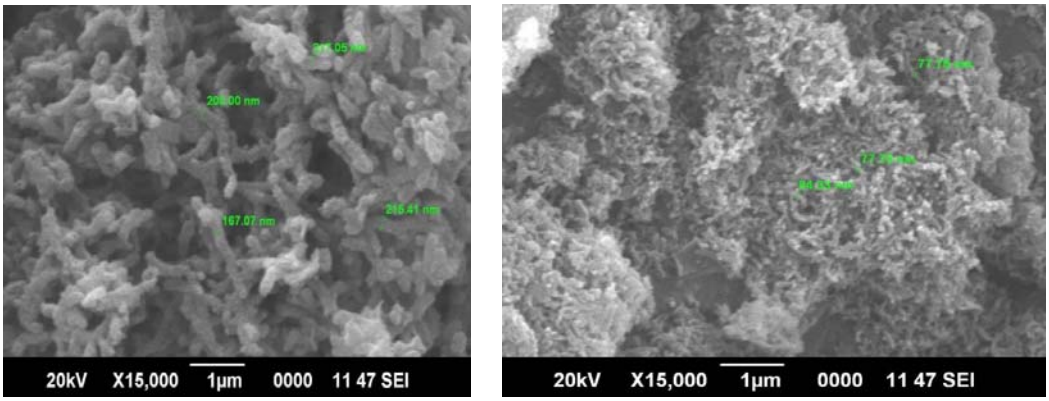

(a) (b)

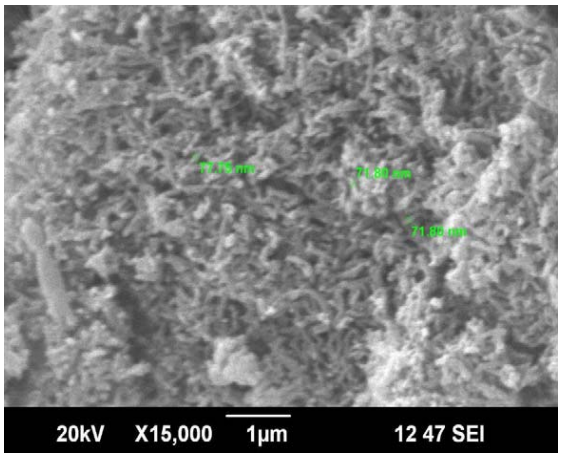

(c)

Figure 1. (a) SEM Micrograph of Bulk PANI-HCl. (b) SEM Micrograph of Nano PANI-HCl. (c) SEM micrograph of Nano PANI-TSA.

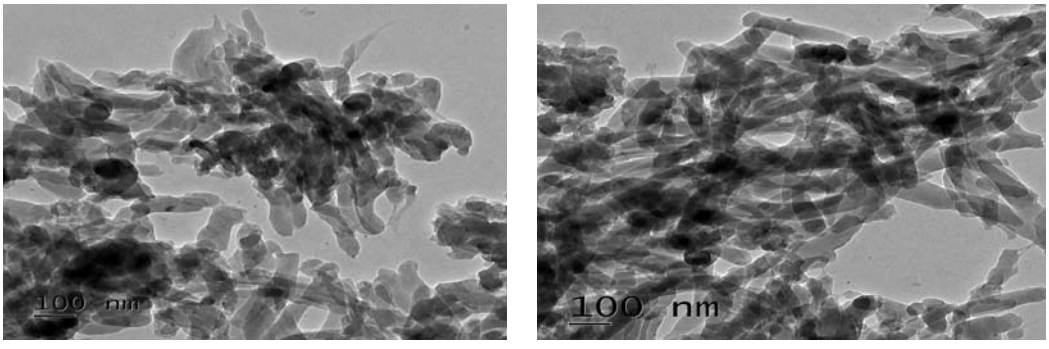

(a) (b)

Figure 2. (a) TEM Micrograph of Nano PANI-HCl. (b) TEM Micrograph of Nano PANI-TSA.

3.3. Fourier Transform Infrared (FTIR) Spectroscopy

Figure 3 shows the FTIR spectra of nano PANI-HCl, nano PANI-TSA, sodium salt of poly(ethylene-co-methacrylic acid) (EMAANa) and EMAANa-PANI (nano PANI-HCl or nano PANI-TSA) blends. The respective bands at 1560 cm^{-1} and 1480 cm^{-1} for nano PANI-HCl and 1557 cm^{-1} and 1477 cm^{-1} for

nano PANI-TSA observed in the spectra are attributed to the C = C stretching of quinoid and benzenoid rings indicating the oxidation state of emeraldine salt PANI [25–28]. The typical peaks at 1293 cm^{-1} and 1240 cm^{-1} in nano PANI-HCl and 1296 cm^{-1} and 1233 cm^{-1} nano PANI-TSA spectra respectively are attributed to the bending vibration of C-N for aromatic amines/imines and C-N^+ stretching vibrations in the polaronic structures (displacement of π electrons) owing to differing conformation or charge configuration suggesting the presence of protonated conducting PANI induced by acid doping of the polymer [29–32]. The strong bands at around 1111 cm^{-1} observed in both nano PANI-HCl and nano PANI-TSA spectra are assigned to C-H in-plane bending vibration considered to be the extent of the degree of delocalization of electrons and thus it is the characteristic peak of PANI [26]. The observed bands at 769 cm^{-1} and 697 cm^{-1}, and 878 cm^{-1} and 800 cm^{-1} for nano PANI-HCl and nano PANI-TSA respectively can be assigned to the aromatic ring out-of-plane deformation vibration bending of C-H bond in the benzene ring and para-distributed aromatic rings indicating polymer formation [32]. Out of plane bending deformation of C-H is observed at 506 cm^{-1} and 500 cm^{-1} in nano PANI-HCl and nano PANI-TSA spectra respectively. The peak at 997 cm^{-1} in nano PANI-TSA can be assigned to SO^{3-} group of the dopant TSA bound to the aromatic rings [27, 28]. The weak and broad signal observed at 3448 cm^{-1} in nano PANI-TSA also is assigned to N-H bond stretching indicating the presence of a secondary amine. This peak is broad and weak such that it is not visible in the nano PANI-HCl spectrum.

The spectra of the ionomer (EMAANa) show a sharp band at 722 cm^{-1} caused by methylene rocking in the pendant backbone. The 1250 cm^{-1} broad peak is attributed to C-O stretching vibrations of COOH groups. The band around 1500 cm^{-1} is due to CO_3 groups. The peak with a wavelength of 1697 cm^{-1} is due to C = O stretching vibrations. The two large peaks and intense peaks at 2844 cm^{-1} and 2920 cm^{-1} are due to CH_3 groups and methyl groups respectively present in the materials [33–36]. The sharp peaks with high intensity observed in the spectra of EMAANa became broad and weak on blending with the different PANIs as seen in the Figure 3. While the EMAANa show sharp and intense peaks, the blends shows weaker peaks. These differences reflect changes in the local environment of the neutralizing cations Na^+ with the PANI, indicating that EMAANa-PANI forms a new structure in the ionic aggregates. The spectrum of the film obtained after blending of PANI with EMAANa, presents all the bands of EMAANa and PANI. However, these bands are not prominent in the EMAANa-PANI-TSA blend, indicating a more interactions between the nano PANI-TSA and EMAANa compared to nano PANI-HCl.

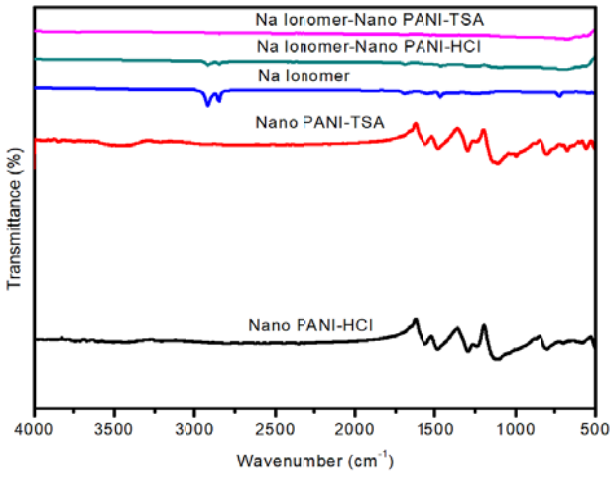

Figure 3. FTIR Spectrum of Nano PANI-HCl, Nano PANI-TSA, Na Ionomer, Na Ionomer-Nano PANI-HCl and Na Ionomer-Nano PANI-TSA.

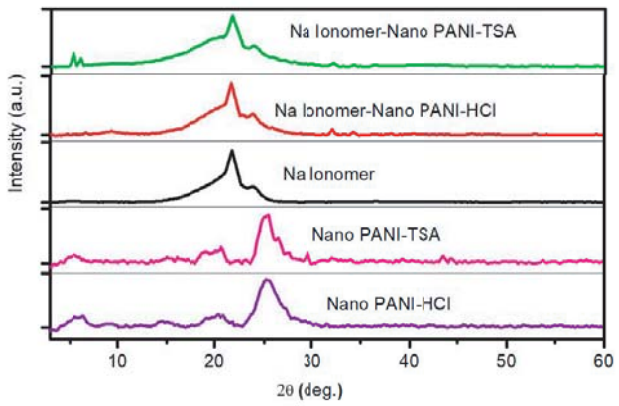

Figure 4. XRD Spectrum of Nano PANI-HCl, Nano PANI-TSA, Na Ionomer, Na Ionomer-Nano PANI-HCl and Na Ionomer-Nano PANI-TSA.

3.4. X-Ray Diffractometry (XRD)

Figure 4 represents the XRD of nano PANI-HCl, nano PANI-TSA, EMAANa, EMAANa-PANI (nano PANI-HCl or nano PANI-TSA) binary blends. The diffraction pattern of nano PANI-HCl are obtained at $2\theta = 6°$, 25° and 31°. The peaks give evidence for the partially crystalline nature of HCl doped PANI with conducting metallic islands separated by large amorphous regions. The diffraction pattern of the toluene sulphonic acid (TSA) doped nano PANI with sharp peaks at $2\theta = 20°$, 25°, 28°, 43° and 44° also indicate the partial crystallinity of the sample. The sharp peak at $2\theta = 29°$ is a characteristic peak indicating the rigidity and well-ordered nature of some portion of PANI sub chains due to interchain packing between poly-cation and TSA anion [25, 29, 37–39]. The peak at $2\theta = 25°$ obtained for the two PANI samples is the characteristic peak of PANI indicating the extent of π conjugation in the polyaniline and sharpness of the peak reveals the degree of order of π conjugation.

The EMAANa pattern shows a single broad peak at around 2θ (21°) indicating that the material is semi crystalline in nature. This peak is known as ionic peak and is attributed to the aggregation of ionic groups in the ionomer resulting in a strong ionic interactions of the metal salts in the ordered structure of the ionic salt groups (ionic crystallites) [40–42]. A second small shoulder-like peak is located at 2θ (24°). This characteristics is also reflected in the two blends. The diffraction pattern of EMAANa-PANI doped with hydrochloric acid (nano PANI-HCl) showed peaks at 2θ (21°, 24°, 32°, 34° and 38°). The diffraction pattern of the toluene sulphonic acid (TSA) doped PANI (nano PANI-TSA)-EMAANa is observed to have bands at 2θ (5°, 6°, 21°, 24°, 32°, and 40°). The sharp peak around (21°) in the neat sodium salt ionomer is very prominent in the two EMAANa-PANI binary blends. The characteristic sharp peak of PANI at around 2θ (21°) is also observed for all two blends. The peaks observed at 21° and a shoulder peak at 24° correspond to the presence of [100] and [200] diffraction peaks of crystal planes of the component crystalline polyethylene crystallites in the EMAA ionomer [43, 44]. These observations are consistent with the degree of polyethylene crystallinity [45, 46]. The peaks observed for the blends are observed to be relatively weaker and broader than that of the neat EMAANa suggesting the extent of intercalation and exfoliation of EMAANa and PANI in the blends indicating a better compatibility between the hydrophobic and the hydrophilic phases in the ionomer blends.

3.5. UV-Visible Spectroscopy (UV-Vis)

The UV-Visible spectra of nano PANI-HCl, nano PANI-TSA, EMAANa, EMAANa-PANI (nano PANI-HCl or nano PANI-TSA) binary blends are shown in Figure 5. Two absorption bands at 277–288 nm and 608–663 nm are obtained for both the samples. The band at 277–288 nm is due to π-π^* transitions in the benzenoid rings of polymer backbone while the band at 608–663 nm is due to exciton absorption of quinoid rings (n-π^*) (inter-band charge transfer associated with excitation of benzoid (HOMO) to quinoid (LUMO) moieties) and a small shoulder-like band at 335 nm attributable to the formation of polaronic/bipolaronic transitions resulting in protonation of the polymer, indicating that the resulting PANIs are in the doped state [29–32]. The continuous absorption peak at 780–790 nm shows free carrier tail, confirming the presence of conducting emeraldine salt phase of the polymer [47]. The slight difference in the absorption bands observed in the two PANI samples might be due to the molecular interaction of the dopants with imine nitrogen of PANI [48] resulting in the slight shift in absorption values. The nano PANI with comparatively larger particles as seen in SEM micrograph which may induce more specular reflection, hence lower absorption and blue shift. This could also influence the conductivity of the samples.

Absorption bands at 335 nm are observed for Na ionomer (EMAANa) and two blends of EMAANa-PANI (nano PANI-HCl or nano PANI-TSA). Two main absorption bands at 277–288 nm and 608–663 nm in all the two PANI samples are not visible in the binary blends. This might be due to exfoliation and homogeneous interaction between ionomer and PANI. Most of the packed products such as organic electronics are prone to degradation due to the incidence of UV radiation. Based on the UV-visible spectroscopic analysis as seen in the absorption bands, it is observed that the blend films have lower UV transmission. Therefore, they can shield better from UV radiation and hence, could be suitable for UV resistant applications.

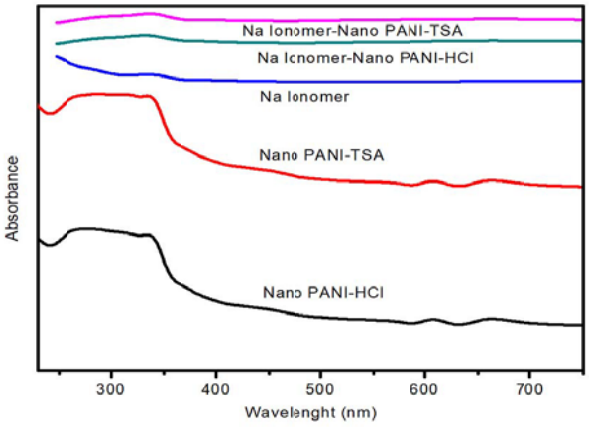

Figure 5. UV-Visible Spectrum of Nano PANI-HCl, Nano PANI-TSA, Na Ionomer, Na Ionomer-Nano PANI-HCl and Na Ionomer-Nano PANI-TSA.

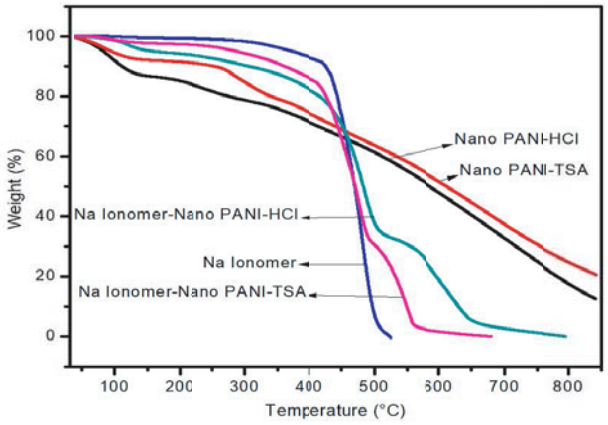

Figure 6. TGA Micrograph of Nano PANI-HCl, Nano PANI-TSA, Na Ionomer, Na Ionomer-Nano PANI-HCl and Na Ionomer-Nano PANI-TSA.

3.6. Thermogravimetric Analysis (TGA)

Figure 6 shows the TGA thermograms nano PANI-HCl, nano PANI-TSA, EMAANa, EMAANa-PANI (nano PANI-HCl or nano PANI-TSA) binary blends. In the first step, approximately 10% and 6% weight loss respectively were observed at the temperature up to 105°C. This is attributable to loss of water molecules and unreacted organic monomers and the free acid trapped in the PANI structure [26, 39, 49]. The second weight losses of about 14% and 9% were observed at temperature in the region of 220°C apparently due to evaporation of dopant acids in PANI samples while the third step of weight loss was marked out at between 500°C and 800°C with 38%, 36% and 18%, 25% weight loss and residues respectively. This possibly represents the oxidative degradation of the PANIs which could be an indication of chemical structure decomposition resulting in chain scission [50]. The thermal behaviour of the two PANI samples are not much different from each other as observed in the thermograms.

The ionomer (EMAANa) exhibits decomposition in two major stages. It showed a 2% weight loss at 300°C. This might be because unlike PANI it does not contain $NH4^+$ ions to release. At 420°C the weight loss of the ionomer was 8%. In between 420°C and 500°C, there was a sharp increase in weight loss (about 96%) giving a residue of 4%. This occurrence may be due to scission in ionic aggregate linkage of the monomeric units of the ionomer [51, 52]. However, at 520°C, the mass of EMAANa was completely decomposed. These decomposition patterns changed with the blending with PANI which tend to retarded the degradation of the molecules of the ionomer at higher temperatures. The improved decomposition temperature showed that the stability of ionomer increased with the introduction of PANI in the blends owing to the reduction in segmental mobility.

3.7. Conductivity Measurements

Sodium ionomer (EMAANa) is an insulating thermoplastic material whose electrical conductivity usually lie around 10^{-17}–10^{-18} Scm^{-1} at room temperature [45]. The electrical conductivity of pelletized bulk PANI-HCl, nano PANI-HCl and nano PANI-TSA are reported to be 0.127 Scm^{-1}, 0.478 Scm^{-1} and 0.824 Scm^{-1} respectively with nano PANI-TSA possessing higher conductivity values. These difference in the electrical conductivities of PANI samples is attributed to a stronger intermolecular interaction between aniline and counteranion molecules when TSA is incorporated [52–55]. The results also show that the nano PANI-HCl is higher than the bulk PANI-HCl. This indicates that PANI in nano dimension are more conducting than in bulk form. The PANI samples were solution blended at various loadings with constant weight of Na ionomer (EMAANa) as presented in Table 1.

The conductivity values of ionomer (EMAANa)-PANI (nano PANI-HCl or nano PANI-TSA) blends as detected by the four-probe method are presented in Table 1. The conductivity values demonstrated

Table 1. DC electrical conductivity of ionomer (EMAANa)-PANI (nano PANI-HCl or nano PANI-TSA) binary blends as a function of weight ratio of PANI of 1.0 g of EMAA-Na.

Weight of PANI (g)	Conductivity (Scm^{-1}) of EMAANa-PANI	
	Nano PANI-HCl	Nano PANI-TSA
0.1	6.33×10^{-4}	6.73×10^{-4}
0.3	6.62×10^{-4}	1.91×10^{-3}
0.5	7.37×10^{-4}	3.25×10^{-3}
0.7	2.15×10^{-3}	4.27×10^{-3}
1.0	2.75×10^{-3}	5.45×10^{-3}
1.2	1.21×10^{-3}	4.31×10^{-3}
1.5	1.16×10^{-3}	5.36×10^{-3}
2.0	9.65×10^{-4}	4.81×10^{-3}

that the conductivity of the blends increased in the order: EMAANa-nano PANI-HCl¡EMAANa-nano PANI-TSA. Though the electrical conductivity of the individual blends did not significantly change with the variation of the PANI content employed in the blending of the ionomer, the gradual increases in conductivity with the content of PANI may be attributed to the quality of intermolecular interactions between PANI and EMAANa causing a possible good and homogenous conductive network. The incidence of percolation threshold (the inflexion point on the dependence of electrical conductivity on filler concentration) occurred at 1 : 1 PANI-ionomer loading where conductivity rose sharply and reached a peak value and then began to experience a decline beyond the same blend ratio [21, 56, 57]. The subsequent decrease in conductivity at higher PANI contents may be due to an observed higher viscosity of the mix and the overwhelming of the ionomer matrix whose weight is constant in the blends. Consequently, the difficulty in the attainment of homogenous dispersion of the PANI in the ionomer matrix, thereby, creating some possible PANI agglomerations and discontinuity in the interfacial interactions between conducting networks of PANI-PANI particles and PANI-ionomer matrix.

3.8. Electromagnetic Interference (EMI) Shielding Effectiveness (SE)

The uses of conducting polymers as microwave absorbers and electromagnetic interference shielding materials have attracted increased attention due to their good electrical conductivity, processability, light weight and non-corrosiveness especially when blended with polymer matrix [50–60]. In this study, the EMI shielding effectiveness of EMAANa-PANI (HCl and TSA) binary blends were measured using a wave-guide coupled to an Agilent Synthesized Sweeper 8375A and a Hewlett-Packard spectrum analyzer 7000. The frequency was scanned from 8.0 to 12.0 GHz (X band) and data taken within the frequency range. It was however observed that the shielding effectiveness of each of the blends is almost independent of the frequency in the measured frequency region. For this reason, in order to do a concise comparison between samples of the composites being studied, a frequency of 8.5 GHz was considered for this analysis as shown in Table 2. All samples were made into thin films after solvent evaporation and drying using compression moulding to press samples into sheets. Samples thickness was 0.29 mm with very negligible variations.

The results indicate that the shielding effectiveness generally increased with the incorporation of PANI in the blends as neat ionomer film exhibited very low EMI shielding effectiveness of 0.3197 dB. Electrical conductivity and or filler content loading are very important parameters with respect to electromagnetic interference (EMI) shielding effectiveness (SE). While conductivity requires connectivity, EMI shielding requires only conductive particles to interact and impede the radiations thus increasing with increase in conductivities and or filler content. The blends consisting of EMAANa-PANI (nano PANI-TSA) showed better shielding effectiveness.

Materials for EMI shielding purposes are typically expected to have a minimum of −20 dB of attenuation, at these values of shielding more than 99% of the incident wave is attenuated ensuring that electronic equipment does not generate, or is not affected by EMI [61]. The values of attenuation

Table 2. Shielding effectiveness of ionomer (EMAANa)-PANI (nano PANI-HCl or nano PANI-TSA) binary blends as a function of weight ratio of PANI to 1.0 g of EMAA-Zn at 8.5 GHz.

Weight of PANI (g)	Shielding Effectiveness (dB) of EMAANa-Nano PANI	
	Nano PANI-HCl	Nano PANI-TSA
1.0	−12.8	−18.7
1.2	−17.7	−22.2
1.5	−18.7	−24.9
2.0	−19.2	−29.1

obtained in this work are lower than the minimum of attenuation that ensures the safety of electronic gadgets nano PANI-HCl. The EMAANa-nano PANI-TSA blends is a promising material for this purpose at the present levels of PANI loading. It is expected that formulations with a higher weight fraction of either of the doped nano PANI can readily go higher than −20 dB especially the EMAANa-nano PANI-TSA blend. Thermal stability of the blend is also expected to improve. However, as the weight fraction of PANI increases, there will be an increase in viscosity; hence, ease of processing and interaction or network interconnectivity between the component blends will be limited. Therefore, it would be important to overcome this limitation by processing the blend formulations via solution blending method.

4. CONCLUSION

The ionomer (EMAANa) matrix used for this work could effectively be dissolved in solvent blends of toluene and 1-butanol at 65°C and its composites with nano PANI could be prepared by solution blending method. Results of UV-visible spectroscopic analyses establish lower UV transmission in the blend films compared to the neat ionomer. Therefore EMAANa-nano PANI composite films could be used for UV shielding applications. The decomposition pattern of EMAANa changed on blending with nano PANI, which tend to retarded the degradation of the molecules of the ionomer at higher temperatures. The improvement in the decomposition temperature of the blends shows that the stability of neat ionomer increased with the introduction of nano PANI, owing to the reduction in segmental mobility. The results of DC electrical conductivity show that the nano PANI-HCl has higher conductivity compared to the bulk PANI-HCl. This indicates that PANI in nano dimension are more conducting than in bulk form. The conductivity was in the order nano PANI-TSA > nano PANI-HCl > bulk PANI-HCl. Among the polymer blends studied, the highest electrical conductivity values is in the 1 : 1 EMAANa-nano PANI-TSA blend. The electromagnetic interference (EMI) shielding effectiveness (SE) of the EMAANa-PANI blends also showed the highest value in EMAANa-nano PANI-TSA blend. The results obtained show that the solution blending is an effective way to improve the processability of electrically conducting nano polyaniline as well as improve the thermal, electrical and EMI SE properties of EMAANa. The values of attenuation obtained in the EMAANa-nano PANI-HCl are lower than the minimum attenuation that ensures the safety of electronic gadgets. The EMAANa-nano PANI-TSA blends are a promising material for EMI shielding. The composite films may be utilized for static charge dissipation, lightweight devices and effective EMI shielding or microwave absorption materials.

REFERENCES

1. Hirasawa, E., Y. Yamamoto, K. Tadano, and S. Yano, "Effect of metal cation type on the structure and properties of ethylene lonomers," *J. Appl. Polym. Sci.*, Vol. 42, 351–362, 1991.
2. Mathias, L. J., Learning Center/ionomer, Accessed June 2, 2018, Available: www.pslc.ws/macrog/Polymer Science.
3. Nandi, A., D. G. Gupta, and A. K. Banthia, "Sulfonated polybutadiene random ionomer as stabilizer for colloidal copper nanoparticles," *Colloids Surf. A: Physicochem Eng. Aspects*, Vol. 197, 119–124, 2002.

4. Capek, I., "Nature and properties of ionomer assemblies II," *Adv. in Colloid Interface Sci.*, Vol. 118, 73–112, 2005.
5. Chodak, I. and I. Krupa, "Percolation effect and mechanical behavior of carbon black filled polyethylene," *J. Mat. Sci. Letters*, Vol. 18, 1457–1459, 1991.
6. Castillo-Ortega, M. M., J. C. Encinas, D. E. Rodriguez, and R. Olayo, "Preparation and characterization of electroconductive polypyrrole-thermoplastic composites," *J. Appl. Polym. Sci.*, Vol. 81, No. 6, 1498–1506, 2001.
7. Carinhana, Jr, D., R. Faez, A. F. Nogueira, and M.-A. De Paoli, "Photoelectrochemical properties of PANI-DBSA/EPDM blends," *Synth. Met.*, Vol. 121, 1569–1570, 2001.
8. Koul, S., R. Chandra, and S. K. Dhawan, "Conducting polyaniline composite: A reusable sensor material for aqueous ammonia," *Sens. Actuat. B*, Vol. 75, 151-9, 2001.
9. Gao, J., J.-M. Sansinena, and H.-L. Wang, "Chemical vapor driven polyaniline sensor/actuators," *Synth. Met.*, Vols. 135–136, 809–810, 2003.
10. Gerard, M., A. Chaubey, and B. D. Malhotra, "Application of conducting polymers to biosensors," *Biosensors & Bioelectronics*, Vol. 17, No. 5, 345–359, 2002.
11. Falcao, E. H. L. and W. M. De Azevedo, "Polyaniline-poly(vinyl alcohol) composite as an optical recording material," *Synth. Met.*, Vol. 128, 149–154, 2002.
12. Faez, R., I. M. Martin, M.-A. De Paoliand, and M. C. Rezende, "Microwave properties of EPDM/PANI-DBSA blends," *Synth. Met.*, Vol. 119, 435-6, 2001.
13. Castillo-Ortega, M. M., T. Del Castillo-Castro, J. C. Encinas, M. Perez-Tello, A. De Paoli Marco, and R. Olayo, "Electrically conducting polyaniline-PBMA composite films obtained by extrusion," *J. Appl. Polym. Sci.*, Vol. 89, 179–183, 2003.
14. Joseph, N., J. Varghese, and M. T. Sebastian, "Self assembled polyaniline nanofibers with enhanced electromagnetic shielding properties," *RSC Adv.*, Vol. 5, 20459–20466, 2015.
15. Gairola, S. P., M. Verma, L. Kumar, M. A. Dar, M. Annapoorni, and R. K. Kotnala, "Enhanced microwave absorption properties in polyaniline and nano-ferrite composite in X-band," *Synth. Met.* Vol. 160, Nos. 21–22, 2315–2318, 2010.
16. Dar, M. A., R. K. Kotnala, V. Verma, J. Shah, W. A. Siddiqui, and M. Alam, "High magneto-crystalline anisotropic core-shell structured $MnO.5ZnO.5Fe_2O_4$/polyaniline nanocomposites prepared by in situ emulsion polymerization," *J. Phys. Chem. C*, Vol. 116, 5277–5287, 2012.
17. Joseph, N., J. Varghese, and M. T. Sebastian, "A facile formulation and excellent electromagnetic absorption of room temperature curable polyaniline nanofiber based inks," *J. Mater. Chem. C*, Vol. 4, 999–1008, 2016.
18. Su, S.-J. and N. Kuramoto, "Synthesis of processable polyaniline complexed with anionic surfactant and its conducting blends in aqueous and organic system," *Synth. Met.*, Vol. 108, No. 2, 121–126, 2000.
19. Barbero, C., H. J. Salavagione, D. F. Acevedo, D. E. Grummelli, F. Garay, G. A. Planes, G. M. Morales, and M. C. Miras, "Novel synthetic methods to produce functionalized conducting polymers I. Polyanilines," *Electrochimica Acta*, Vol. 49, Nos. 22–23, 3671–3686, 2004.
20. Yang, J. P., R. J. Planes, A. Pron, and M. Nechtschein, "Preparation of low density polyethylene-based polyaniline conducting polymer composites with low percolation threshold via extrusion," *Synth. Met.*, Vol. 93, 169–173, 1998.
21. Castillo-Ortega, M. M., D. E. Rodriguez, J. C. Encinas, M. Plascencia, F. A. Mendez-Velarde, and R. Olayo, "Conductometric uric acid and urea biosensor prepared from electroconductive polyaniline-poly(n-butyl methacrylate) composites," *Sens. Actuat. B*, Vol. 85, 19–25, 2002.
22. Wang, Y., H.-Q. Xie, Y. Cai, and J. Guo, "Synthesis and properties of polyaniline/sodium and zinc ionomer composites," *Polym. J.*, Vol. 29, No. 11, 875–880, 1997.
23. Xie, H.-Q., Q.-L. Pu, and D. Xie, "Preparation of conductive polyaniline-sulfonated EPDM ionomer composites from in situ emulsion polymerization and study of their properties," *J. Appl. Polym. Sci.*, Vol. 93, 2211–2217, 2004.

24. Morgan, H., P. J. S. Foot, and N. W. Brooks, "The effects of composition and processing variables on the properties of thermoplastic polyaniline blends and composites," *J. Mat. Sci.*, Vol. 36, No. 22, 5369–5377, 2001.
25. Mathew, H., V. S. Punnackal, S. Kuriakose, B. S. Kumari, and A. Manuel, "Synthesis and electrical characterization of polyaniline-multiwalled carbon nanotube composites with different dopants," *Int. J. Sci. Res. Pub.*, Vol. 3, No. 8, 1–10, 2013.
26. Kumar, A., V. Kumar, M. Kumar, and K. Awasthi, "Synthesis and characterization of hybrid PANI/MWCNT nanocomposites for EMI applications," *Polymer Composites*, 2017, doi 10.1002/pc.24418.
27. Abdullah, E. T., R. S. Ahmed, S. M. Hassan, and A. N. Naje, "Synthesis and characterization of PANI and polyaniline/multi walled carbon nanotube composite," *Int. J. Application or Innovation Eng. Mgt.*, Vol. 4, No. 9, 130–134, 2015.
28. Ratheesh, R. and K. Viswanathan, "Chemical polymerization of aniline using para-toluene sulphonic acid," *IOSR J. Appl. Phy.*, Vol. 6, No. 1, 1–9, 2014.
29. Rafeeq, S. N. and W. Z. Khalaf, "Preparation, characterization and electrical conductivity of doped polyaniline with (HCL and P-TSA)," *The 5th International Scientific Conference for Nanotechnology and Advanced Materials and Their Applications ICNAMA*, 3–4, 2015.
30. Chakraborty, G., K. Gupta, D. Rana, and A. K. Meikap, "Effect of multiwalled carbon nanotubes on electrical conductivity and magnetoconductivity of polyaniline," *Adv. Nat. Sci.: Nanosci. Nanotechnol.*, Vol. 3, 1–8, 2012.
31. Babu, V. J., S. Vempati, and S. Ramakrishna, "Conducting polyaniline-electrical charge transportation," *Mat. Sci. Applications*, Vol. 4, 1–10, 2013.
32. Bachhav, S. G. and D. R. Patil, "Synthesis and characterization of polyaniline-multiwalled carbon nanotube nanocomposites and its electrical percolation behavior," *Amer. J. Mat. Sci.*, Vol. 5, No. 4, 90–95, 2015.
33. Painter, P. C., B. A. Brozoski, and M. M. Coleman, "FTIR studies of calcium and sodium ionomers derived from an ethylene-methacrylic acid and copolymer," *J. Polym. Sci.: Polym. Phy.*, Vol. 20, No. 6, 1069–1080, 1982.
34. Kutsumizu, S., H. Hara, H. Tachino, K. Shimabayashi, and S. Yano, "Infrared spectroscopic study of the binary blends of sodium and zinc salt ionomers produced from poly(ethylene-co-methacrylic acid)," *Macromolecules*, Vol. 32, No. 19, 6340–6347, 1999.
35. Reynolds, P. J. and A. Surlyn®, "Ionomer as a self-healing and self-sensing composite," MRes Thesis, Department of Metallurgy and Materials, University of Birmingham, UK, 2012.
36. Ramos, J. M., M. T. de M Cruz, A. C. Costa, Jr., O. Versiane, and C. A. T. Soto, "Fourier transform infrared spectrum: Vibrational assignments using density functional theory and natural bond orbital analysis of the bis (guanido acetate) nickel (II) complex," *ScienceAsia*, Vol. 37, 247–255, 2011.
37. Abdullah, E. T., S. M. Hassan, and R. S. Ahmed, "Electrical properties of polyaniline/functionalized multi walled carbon nanotubes nanocomposite," *Int. J. Current Eng. Technol.*, Vol. 6, No. 2, 617–621, 2016.
38. Wu. T.-M. and Y.-W. Lin, "Doped polyaniline/multi-walled carbon nanotube composites: Preparation, characterization and properties," *Polym.*, Vol. 47, 3576–3582, 2006.
39. Gajendran, P. and R. Saraswathi, "Polyaniline-carbon nanotube composites," *Pure Appl. Chem.*, Vol. 80, No. 11, 2377–2395, 2008.
40. Kutsumizu, S., H. Hara, H. Tachino, K. Shimabayashi, and S. Yano, "Infrared spectroscopic study of the binary blends of sodium and zinc salt ionomers produced from poly(ethylene-co-methacrylic acid)," *Macromolecules*, Vol. 32, 6340–6347, 1999.
41. Pineri, M. and A. Eisenberg, "Structure and properties of ionomers," *Nato Science Series C, Mathematical and Physical Sciences D*, Vol. 198, Reidel Dordrecht, Netherlands, 1987.
42. Schlick, S., *Ionomers: Characterization, Theory and Applications*, Taylor and Francis, CRC Press, Boca Raton, FL, 1996.

43. Gazotti, Jr., W. A., G. Casalbore-Miceli, S. Mitzakoff, A. Geri, M. C. Gallazzi, and M.-A. De Paoli, "Conductive polymer blends as electrochromic materials," *Electrochimica Acta*, Vol. 44, 1965–1971, 1999.
44. Shah, R. K. and D. R. Paul, "Comparison of nanocomposites prepared from sodium, zinc and lithium ionomers of ethylene/methacrylic acid copolymers," *Macromolecules*, Vol. 39, No. 9, 3327–3336, 2006.
45. Kutsumizu, S., K. Tadano, Y. Matsuda, M. Goto, H. Tachino, H. Hara, E. Hirasawa, H. Tagawa, Y. Muroga, and S. Yano, "Investigation of microphase separation and thermal properties of noncrystalline ethylene ionomers. 2. IR, DSC and dielectric characterization," *Macromolecules*, Vol. 33, No. 24, 9044–9053, 2000.
46. Ray, S., A. J. Easteal, R. P. Cooney, and N. R. Edmonds, "Structure and properties of melt-processed PVDF/PMMA/polyaniline blends," *Mat. Chem. Phy.*, Vol. 113, 829–838, 2009.
47. Kulkarni, M. V. and B. B. Kale, "Development of optical pH sensor using conducting polyaniline-wrapped multiwalled carbon nanotubes (PANI-MWCNTs) nanocomposite," *IMCS 2012 — The 14th International Meeting on Chemical Sensors*, 2012, DOI 10.5162/IMCS2012/P1.3.2.
48. Khalid, M., M. A. Tumelero, I. S. Brandt, V. C. Zoldan, J. J. S. Acuna, and A. A. Pasa, "Electrical conductivity studies of polyaniline nanotubes doped with different sulfonic acids," *Indian J. Mat. Sci.*, Article ID 718304, 2013, doi.org/10.1155/2013/718304.
49. Yılmaz, F. and Z. Kuqukyavuz, "Conducting polymer composites of multiwalled carbon nanotube filled doped polyaniline," *J. Appl. Polym. Sci.*, Vol. 111, 680–684, 2009.
50. Zhang, J.-Q., C.-M. Shi, T.-Z. Ji, G.-L. Wu, and K.-C. Kou, "Preparation and microwave absorbing characteristics of multi-walled carbon nanotube/chiral-polyaniline composites," *Open J. Polym. Chem.*, Vol. 4, 62–72, 2014.
51. Pazhanisamy, P. and B. S. R. Reddy, "Synthesis and characterization of methacrylamidopropyltrimethylammonium chloride and N-substituted acrylamide ionomers," *Express Polym Letters*, Vol. 1, No. 11, 740–747, 2007.
52. Li, D. and G. S. Sur, "Comparison of poly(ethylene-co-acrylic acid) loaded Zn^{2+}-montmorillonite nanocomposites and poly(ethylene-co-acrylic acid) zinc salt," *J. Ind. Eng. Chem.*, Vol. 20, No. 5, 3122–3127, 2014.
53. Kutsumizu, S., Y. Hashimoto, H. Hara, H. Tachino, E. Hirasawa, and S. Yano, "DC conduction properties of a model ethylene-methacrylic acid ionomer," *Macromol*, Vol. 27, No. 7, 1781–1787, 1994.
54. Das, N. C., S. Yamazaki, M. Hikosaka, T. K. Chaki, D. Khastgir, and A. Chakraborty, "Electrical conductivity and electromagnetic interference shielding effectiveness of polyaniline ethylene vinyl acetate composites," *Polym. Int.*, Vol. 54, 256–259, 2005.
55. Chutia, P. and A. Kumar, "Electrical, optical and dielectric properties of HCl doped polyaniline nanorods," *Physica B*, Vol. 436, 200–207, 2014.
56. Zilberman, M., A. Siegmann, and M. Narkis, "Conductivity and structure of melt-processed polyaniline binary and ternary blends," *Polym. Adv. Technol.*, Vol. 11, 20–26, 2000.
57. Terlemezyan, L., M. Mihailov, and B. Ivanova, "Electrically conductive polymer blends comprising polyaniline," *Polym. Bull.*, Vol. 29. 283–287, 1992.
58. Wang, Y., "Microwave absorbing materials based on polyaniline composites: A review," *Int. J. Mat. Res.*, Vol. 105, No. 1, 3–12, 2014.
59. Thomassin, J. M., C. Jerome, T. Pardoen, C. Bailly, I. Huynen, and C. Detrembleur, "Polymer/carbon based composites as electromagnetic interference (EMI) shielding materials," *Mat. Sci. Eng. Reports*, Vol. 74, No. 7, 211–232, 2013.
60. John, H., R. M. Thomas, J. Jacob, K. T. Mathew, and R. Joseph, "Conducting polyaniline composites as microwave absorbers," *Polym. Comp.*, Vol. 28, No. 5, 588–582, 2007.
61. Schmitza, D. P., L. G. Ecco, S. Dulb, E. C. L. Pereirac, B. G. Soares, G. M. O. Barraa, and A. Pegoretti, "Electromagnetic interference shielding effectiveness of ABS carbon-based composites manufactured via fused deposition modelling," *Mater. Today Commun.*, Vol. 15, 70–80, 2018.